Journal of Dental Sciences

Volume 21 | Issue 2 Article 31

2026

Cancer-associated fibroblast-derived interleukin-6 as a key driver of epithelial–mesenchymal transition and metastasis in oral squamous cell carcinoma

Soon Chul Heo

Jihye Ryu

Bo Ram Keum

Moon-Kyoung Bae

Hyung Joon Kim

Journal of Dental Sciences 21 (2026) 932–941

Available online at https://jds.ads.org.tw/journal/

Digital Commons

journal homepage: https://jds.ads.org.tw/journal/

Original Article

Cancer-associated fibroblast-derived interleukin-6 as a key driver of epithelial–mesenchymal transition and metastasis in oral squamous cell carcinoma

Soon Chul Heo [a,b†], Jihye Ryu [c†], Bo Ram Keum [a], Moon-Kyoung Bae [a], Jae-Yeol Lee [d], Hyung Joon Kim [a*]**

[a] *Department of Oral Physiology, Periodontal Diseases Signaling Network Research Center, Dental and Life Science Institute, School of Dentistry, Pusan National University, Yangsan 50612, Republic of Korea*

[b] *Institute of Tissue Regeneration Engineering (ITREN), Mechanobiology Dental Medicine Research Center, Dankook University, Cheonan 31116, Republic of Korea*

[c] *Department of Oral and Maxillofacial Surgery, Pusan National University Dental Hospital, Yangsan 50612, Republic of Korea*

[d] *Department of Oral and Maxillofacial Surgery, Dental and Life Science Institute & Dental Research Institute, School of Dentistry, Pusan National University, Yangsan 50612, Republic of Korea*

Received 7 July 2025; Final revision received 7 August 2025
Available online 1 April 2026

KEYWORDS
Cancer-associated fibroblast;
Epithelial–mesenchymal transition;
Interleukin-6;
Oral squamous cell carcinoma

Abstract *Background/purpose:* Oral squamous cell carcinoma (OSCC) is a highly metastatic cancer with a poor prognosis, partly driven by epithelial–mesenchymal transition (EMT). Although several cytokines have been implicated in OSCC progression, the specific role of cancer-associated fibroblast (CAF)-derived interleukin-6 (IL-6) in EMT and metastasis remains poorly understood. This study investigated the contribution of CAF-derived IL-6 to the promotion of EMT and metastasis in OSCC.

Materials and methods: Conditioned media from gingival fibroblasts (GF) treated with OSCC-conditioned media (SCC25-GF CM) were analyzed using secretomic and functional assays. EMT marker expression, migration, and invasion were evaluated by RT-qPCR, Western blotting, immunofluorescence, and an IL-6 neutralizing antibody.

* Corresponding author. Department of Oral Physiology, School of Dentistry, Pusan National University, 49 Busandaehak-ro, Yangsan 50612, Republic of Korea.

** Corresponding author. Department of Oral and Maxillofacial Surgery, Dental and Life Science Institute & Dental Research Institute, School of Dentistry, Pusan National University, 49 Busandaehak-ro, Yangsan 50612, Republic of Korea.

E-mail addresses: omsljy@pusan.ac.kr (J.-Y. Lee), hjoonkim@pusan.ac.kr (H.J. Kim).

† These authors contributed equally to this work.

https://doi.org/10.1016/j.jds.2025.08.019

Results: SCC25-GF CM significantly downregulated E-cadherin and upregulated N-cadherin, vimentin, and Snail expression, indicating EMT induction. Secretome analysis revealed elevated levels of multiple EMT- and metastasis-associated factors, including stromelysin-1, glia-derived nexin, tenascin, procathepsin L, and IL-6, in SCC25-GF CM. IL-6 neutralization reduced EMT marker expression, migration, and invasion in SCC25 cells, demonstrating that IL-6 is a key driver of CAF-mediated EMT in OSCC.
Conclusion: These findings indicate that IL-6 is a central mediator of CAF-induced EMT and contributes to the metastatic potential of OSCC, highlighting IL-6 as a promising therapeutic target.

Introduction

Squamous cell carcinoma (SCC) is the most prevalent form of head and neck cancer, accounting for over 90 % of all oral cavity malignancies. Oral squamous cell carcinoma (OSCC) presents significant clinical challenges due to its aggressive nature and poor prognosis.[1–3] According to recent data from the Global Cancer Observatory, the annual mortality rate associated with oral cavity cancers is projected to rise dramatically, from 178,000 deaths in 2020 to 263,000 by 2040, reflecting a 47 % increase.[4] OSCC is associated with a five-year survival rate of less than 60 %, primarily due to its tendency for local recurrence and distant metastasis, which are hallmarks of advanced disease.[5] These poor outcomes have prompted intensive research into the molecular and cellular mechanisms underlying OSCC progression, with a particular focus on identifying factors involved in recurrence and metastasis. Such insights hold the potential to enable earlier diagnosis and guide targeted therapies development.

Epithelial-mesenchymal transition (EMT), a biological process in which epithelial cells lose their cell–cell adhesion properties and acquire mesenchymal traits, thereby acquiring enhanced migratory and invasive capabilities,[6] plays a central role in the metastatic cascade of OSCC. In OSCC, EMT enables tumor cells to invade surrounding tissue and enter the vasculature, facilitating distant metastasis. The tumor microenvironment (TME) significantly influences the EMT process through its various components, including growth factors, cytokines, and the extracellular matrix (ECM), which act as key effectors. These EMT-inducing signals reprogram cellular behavior and promote tumor progression and dissemination. Markers such as E-cadherin (encoded by *CDH1*) are typically downregulated during EMT, correlating with poor differentiation, advanced TNM stage, and frequent metastasis.[7,8] Conversely, mesenchymal markers such as N-cadherin (encoded by *CDH2*) and vimentin, along with transcription factors including Twist, ZEB1/2, and Snail, are upregulated, facilitating cellular migration and invasion.[9–11] These changes indicate adverse prognostic factors and are also associated with larger tumors, increased metastasis, and poor overall survival. Collectively, these markers reflect the dynamic changes that drive EMT and underscore their significance in OSCC progression.

Cancer-associated fibroblasts (CAFs), a dominant stromal component of the tumor microenvironment (TME), are critical mediators of oral squamous cell carcinoma (OSCC) progression. They originate from resident stromal cells, such as gingival fibroblasts, which undergo activation and phenotypic reprogramming in response to tumor-derived factors.[12,13] Upon activation, CAFs acquire distinct characteristics, including the expression of mesenchymal markers such as alpha-smooth muscle actin (αSMA) and vimentin and exhibit increased secretion of ECM components and cytokines that drive TME remodeling.[14–16] This reprogramming is facilitated by proinflammatory and tumor-derived signals. Previous studies, including our own, have demonstrated that OSCC-conditioned medium (OSCC CM) induces the differentiation of gingival fibroblasts into CAFs. Notably, cytokines such as CXCL1 play a pivotal role in mediating this transition, creating a positive feedback loop that enhances tumor–stromal interactions.[17] CAFs further establish a supportive niche for OSCC by promoting tumor cell proliferation, migration, invasion, and metastasis. These contributions highlight the dynamic and reciprocal interactions between cancer cells and stromal components, positioning CAFs as a central focus in understanding OSCC progression and developing potential therapeutic strategies. Despite these insights, the precise molecular mechanisms and specific factors secreted by CAFs that drive metastatic processes within the TME remain inadequately characterized, emphasizing the need for further investigation into the complex interplay between CAFs and tumor cells.

Cytokines such as transforming growth factor-beta, tumor necrosis factor-alpha, and monocyte chemoattractant protein-1 have been extensively studied for their contributions to EMT.[18–20] Among these, interleukin-6 (IL-6) has garnered significant attention due to its multifaceted role in OSCC.[21] IL-6 is a pleiotropic cytokine that activates the JAK/STAT3 signaling pathway, inducing the expression of mesenchymal markers while suppressing epithelial traits, thereby promoting tumor cell migration and invasion.[22,23] In addition to its role in EMT, IL-6 contributes to immune

modulation, stromal remodeling, and angiogenesis, further accelerating tumor progression.[24–26] However, the precise cellular sources of IL-6 within the TME, the mechanisms regulating its secretion, and its precise impact on OSCC progression remain poorly understood. This underscores the importance of elucidating IL-6's role in the TME to evaluate its potential as a therapeutic target in OSCC treatment.

This study builds on our previous findings that identified CXCL1 as a key inducer of CAF differentiation in gingival fibroblasts exposed to OSCC-CM. Here, we investigated the functional role of these differentiated CAFs in OSCC progression, focusing on CAF-secreted IL-6 as a potential driver of EMT. Using secretomics and functional assays, we characterized the proteomic landscape of CAF-CM and identified critical cytokines involved in promoting EMT in OSCC. Ultimately, our findings highlight IL-6 as a central mediator of EMT and metastasis and provide new insights into its potential as a therapeutic target in OSCC.

Materials and methods

Reagents

Minimum essential medium with alpha modifications (α-MEM), Dulbecco's Modified Eagle Medium (DMEM), RPMI 1640 Medium, and Dulbecco's phosphate-buffered saline (DPBS) were obtained from Welgene, Inc. (Daegu, Republic of Korea). Fetal bovine serum (FBS), trypsin—EDTA, and penicillin-streptomycin (P/S) were purchased from Gibco (Thermo Fisher Scientific Inc., Waltham, MA, USA). Antibodies against vimentin, β-actin, E-cadherin, and N-cadherin were obtained from Cell Signaling Technology (Danvers, MA, USA). Neutralizing monoclonal antibodies against human IL-6 and mouse control IgG were purchased from InvivoGen (San Diego, CA, USA).

Cell culture

Gingival fibroblasts (GF) were purchased from ScienCell (California, USA) and cultured in α-MEM supplemented with 10 % FBS and 1 % P/S. SCC25 cells were purchased from the American Type Culture Collection (Manassas, VA, USA) and cultured in DMEM supplemented with 10 % FBS and 1 % P/S. All cells were maintained at 37 °C in 5 % CO2 and passaged upon reaching 90 % confluence.

Preparation and application of conditioned medium (CM)

For SCC25 CM preparation, SCC25 cells were seeded in 150-mm dishes and grown to sub-confluence. After washing twice with DPBS to remove residual serum, cells were incubated in 20 mL of serum-free medium for 24 h. The collected medium was centrifuged at 3000×*g* for 10 min to remove cell debris and filtered through a 0.2 μm syringe filter (Sartorius, Goettingen, Germany). For GF CM preparation, GF were grown to sub-confluence, washed twice with DPBS, and incubated in serum-free medium either alone (Control GF CM) or supplemented with 50 % SCC25 CM (SCC25-GF CM) for 48 h. After this incubation, the cells were thoroughly washed with DPBS to remove residual SCC25 CM and then cultured in fresh serum-free medium for an additional 24 h. The resulting CM was processed as described for SCC25 CM. Prepared Control GF CM and SCC25-GF CM were subsequently applied to SCC25 cells.

Enzyme-linked immunosorbent assay (ELISA)

IL-6 protein levels in conditioned media were quantified using the ELISA MAX™ Deluxe Set Human IL-6 (BioLegend, San Diego, CA, USA) according to the manufacturer's instructions. Absorbance was measured at 450 nm using an Opsys MR microplate reader.

Western blotting

Protein lysates were extracted using RIPA buffer (50 mM Tris, pH 8.0, 150 mM NaCl, 0.5 % sodium deoxycholate, 1 mM EGTA, 1 % Triton X-100, 10 mM NaF, PMSF, and complete protease inhibitor cocktail). Equal amounts of protein (20 μg) were separated by SDS-PAGE (10 % or 15 % gel) and transferred to nitrocellulose membranes. Membranes were blocked with 5 % skim milk for 1 h and incubated overnight at 4 °C with primary antibodies. After washing, membranes were incubated with horseradish peroxidase-conjugated secondary antibodies for 1 h at room temperature. Protein bands were visualized using an enhanced chemiluminescence reagent (Amersham Pharmacia Biotech Ltd.). β-actin was used as a loading control.

Reverse transcription quantitative PCR (RT-qPCR)

Total RNA was extracted using the RNeasy Mini Kit (Qiagen) and reverse transcribed into cDNA using Superscript II (Invitrogen, Waltham, MA, USA). For RT-qPCR, 50 ng of cDNA was amplified using SYBR Green PCR Master Mix (Applied Biosystems, Foster City, CA, USA) and analyzed on an AB7500 system (Applied Biosystems) for 40 cycles. Experiments were performed in triplicate, and expression levels were normalized to *ACTB*. The $2^{-\Delta\Delta Ct}$ method was used for data analysis. The primer sequences used were as follows: *CDH1*, 5′- GCCTCCTGAAAAGAGAGTGGAAG-3′, 5′-TGGCAGTGTCTCTCCAAATCCG-3′; *CDH2*, 5′-CCTCCAGAGTTTACTGCCATGAC-3′, 5′-GTAGGATCTCCGCCACTGATTC-3′; *Vimentin*, 5′-AGGCAAAGCAGGAGTCCACTGA-3′, 5′- ATCTGGCGTTCCAGGGACTCAT-3′; *Snai1*, 5′- TGCCCTCAAGATGCACATCCGA-3′, 5′- GGGACAGGAGAAGGGCTTCTC-3'; *ACTB*, 5′-ACTCTTCCAGCCTTCCTTCC-3′, 5′-TGTTGGCGTACAGGTCTTTG-3′.

Immunocytochemistry

Cells were fixed with 4 % paraformaldehyde and permeabilized with 0.2 % Triton X-100. After blocking with 5 % BSA, cells were incubated with primary antibodies against E-cadherin, N-cadherin, or vimentin, followed by fluorescently labeled secondary antibodies (Alexa Fluor 488 or Alexa Fluor 555, Thermo Fisher Scientific). Nuclei were counterstained with DAPI (Sigma—Aldrich). Images were acquired using a confocal microscope (LSM 700; Carl Zeiss).

Liquid chromatography–tandem mass spectrometry (LC-MS/MS) analysis

Protein concentrations were measured using the Pierce BCA Protein Assay Kit (Thermo Fisher Scientific). For digestion, 100 μg of each protein sample was processed using the Filter-Aided Sample Preparation (FASP) method. Samples were reduced with Tris (2-carboxyethyl) phosphine (TCEP), alkylated with iodoacetic acid, and digested with trypsin at a 1:50 enzyme-to-protein ratio at 37 °C for 18 h. Peptides were desalted using a C18 spin column and eluted with 80 % acetonitrile containing 0.1 % formic acid. Peptide samples were analyzed using a SCIEX TripleTOF 5600+ mass spectrometer coupled to an Ekspert NanoLC 425 system (Eksigent). Chromatographic separation was carried out using a ChromXP C18CL analytical column at 40 °C. Peptides were eluted using a linear acetonitrile gradient in 0.1 % formic acid for 37 min. Data were acquired in SWATH mode using 100 variable windows, with a scan range of 400–1250 m/z and a cycle time of 2.8 s. Raw spectral data were processed using the UniProt Human Reference Library. Proteins were identified with a 1 % false discovery rate (FDR) threshold. Differential expression analysis was conducted in R (version 3.6.0) using log-transformed values. Statistical significance was determined using paired t-tests followed by the Benjamini-Hochberg correction for multiple comparisons.

Transwell invasion assay

SCC25 cells (5×10^4 cells/well) were seeded in serum-free medium in the upper chamber of 8 μm pore-size transwell inserts (SPL, Republic of Korea) coated with Matrigel. The lower chamber contained either serum-free medium or CM. After 16 h, non-invasive cells were removed, and invasive cells were fixed, stained with 0.1 % crystal violet, and counted under a microscope (Nikon, Eclipse Ts2).

Scratch wound migration assay

SCC25 cells were cultured to confluence in a 24-well plate and scratched with a pipette tip to create a wound. Cells were then incubated in serum-free medium or CM. After 16 h, wound closure was assessed by measuring the area covered by migrating cells relative to the original wound area.

Interleukin-6 neutralization

To inhibit IL-6 activity, 100 μg/mL of an IL-6 neutralizing antibody (nIL-6 Ab) was added to SCC25-GF CM. Mouse IgG was used as a control.

Statistical analysis

Statistical comparisons were performed using Student's *t*-tests or one-way ANOVA with Bonferroni post hoc tests for multiple group comparisons. Results were considered statistically significant at $P < 0.05$ ($^{*}P < 0.05$, $^{**}P < 0.01$, $^{***}P < 0.001$) and are presented as mean ± SD from at least three independent experiments.

Results

Conditioned medium from SCC25-activated gingival fibroblasts enhances epithelial–mesenchymal transition-associated changes in SCC25 cells

SCC25 cells were treated with conditioned media to evaluate changes associated with EMT. Control GF-conditioned medium (Con-GF CM) was derived from non-activated GF, while SCC25-GF CM was obtained from GF activated with SCC25-CM. These CM were applied to SCC25 cells, and changes in EMT-related markers were analyzed. E-cadherin (*CDH1*) served as an epithelial marker, while N-cadherin (*CDH2*), *vimentin*, and *Snai1* served as mesenchymal markers. RT-qPCR showed significant downregulation of *CDH1* expression and upregulation of *CDH2*, *vimentin*, and *Snai1* in SCC25-GF CM-treated cells compared to both the Con-GF CM-treated and control groups (Fig. 1A). Western blot analysis confirmed these findings at the protein level: E-cadherin protein levels were reduced, while N-cadherin and vimentin levels were elevated in SCC25-GF CM-treated cells (Fig. 1B). Immunofluorescence imaging further supported these results. E-cadherin was strongly localized at cell–cell junctions in control cells but was significantly reduced in SCC25-GF CM-treated cells. In contrast, N-cadherin and vimentin displayed increased fluorescence intensity and were predominantly localized in the cytoplasm of SCC25-GF CM-treated cells (Fig. 1C). These results highlight both expression-level and spatial changes in key EMT markers following SCC25-GF CM treatment.

Conditioned medium from SCC25-activated gingival fibroblasts promotes migratory and invasive traits in SCC25 cells

To assess the functional impact of SCC25-GF CM on EMT, scratch wound migration and Transwell invasion assays were conducted. In the scratch wound assay, Con-GF CM treatment modestly increased wound closure compared to the control group, while SCC25-GF CM treatment significantly enhanced wound closure (Fig. 2A). Quantitative analysis confirmed that SCC25-GF CM-treated cells exhibited significantly higher wound closure rates than both control and Con-GF CM-treated groups (Fig. 2B). In the Transwell invasion assay, Con-GF CM-treated cells showed an increased number of invasive cells compared to controls, whereas SCC25-GF CM-treated cells displayed a markedly enhanced invasive capacity (Fig. 2C). Quantification of invasive cells per field further demonstrated that SCC25-GF CM induced significantly greater invasiveness than Con-GF CM (Fig. 2D). These results suggest that SCC25-GF CM contains a higher concentration of EMT-promoting factors, contributing to the increased migratory and invasive characteristics of SCC25 cells.

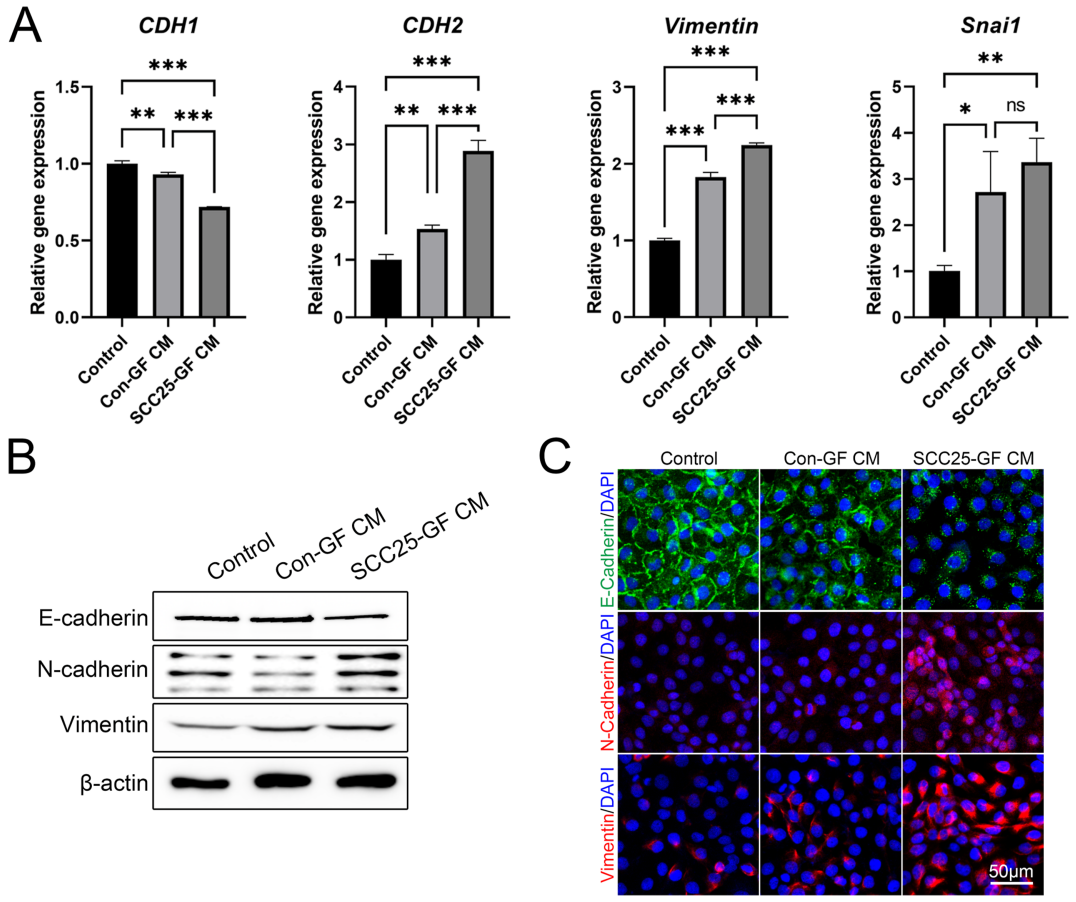

Figure 1 Analysis of EMT marker expression in SCC25 cells treated with conditioned media from gingival fibroblasts. (A) Quantitative RT-qPCR analysis of *CDH1*, *CDH2*, *Vimentin*, and *Snai1* mRNA levels in SCC25 cells treated with control gingival fibroblast-conditioned medium (Con-GF CM) or SCC25-activated gingival fibroblast-conditioned medium (SCC25-GF CM) for 24 h. (B) Western blot analysis of E-cadherin, N-cadherin, and vimentin protein levels in SCC25 cells treated with either Con-GF CM or SCC25-GF CM. *ACTB* was used as a loading control. (C) Immunofluorescence staining of E-cadherin, N-cadherin, and vimentin in SCC25 cells treated with Con-GF CM or SCC25-GF CM. Nuclei were counterstained with DAPI. Scale bars = 50 μm. Data are presented as mean ± SD. *$P < 0.05$, **$P < 0.01$, and ***$P < 0.001$ by one-way ANOVA. Con-GF CM, conditioned medium from non-activated gingival fibroblasts; SCC25-GF CM, conditioned medium from SCC25-activated gingival fibroblasts; ns, not significant.

Uncovering interleukin-6 as an epithelial–mesenchymal transition inducer through secretome profiling

To identify EMT-promoting proteins in SCC25-GF CM, secretome profiling was performed using LC-MS/MS. A total of 715 proteins were identified, among which 262 were upregulated and 453 were downregulated in SCC25-GF CM compared to Con-GF CM. Notably, several proteins known to be involved in tumor metastasis and EMT, including stromelysin-1 (*MMP3*), glia-derived nexin (*SERPINE2*), tenascin (*TNC*), procathepsin L (*CTSL*), and IL-6, were among the most upregulated factors (Fig. 3A and Table S1). Given the well-established role of IL-6 in EMT regulation, we focused on IL-6. To validate the LC-MS/MS findings, RT-qPCR was performed to assess IL-6 gene expression in Con-GF and SCC25-GF cells. IL-6 expression was significantly higher in SCC25-GF cells compared to Con-GF cells (Fig. 3B). To further confirm these findings at the protein level, IL-6 concentrations in Con-GF CM and SCC25-GF CM were quantified using ELISA. Consistent with the transcript data, SCC25-GF CM contained significantly higher IL-6 protein levels compared to Con-GF CM (Fig. 3C). These results confirm that IL-6 is upregulated in SCC25-GF CM and may serve as a key inducer of EMT in this context.

Neutralization of interleukin-6 mitigates epithelial–mesenchymal transition marker alterations

To confirm the role of IL-6 as a key driver of EMT, an nIL-6 Ab was added to inhibit IL-6 activity in SCC25-GF CM. RT-qPCR analysis revealed that treatment with SCC25-GF CM with control IgG significantly reduced *CDH1* expression and increased the expression of *CDH2*, *vimentin*, and *Snai1*. However, the addition of nIL-6 significantly attenuated these effects, lessening *CDH1* downregulation and mitigating the upregulation of *CDH2* and *vimentin* (Fig. 4A). Western blot analysis further supported these findings. While SCC25-GF CM with control IgG showed decreased E-cadherin levels and elevated N-cadherin and vimentin levels, the addition of nIL-6 Ab reversed these changes,

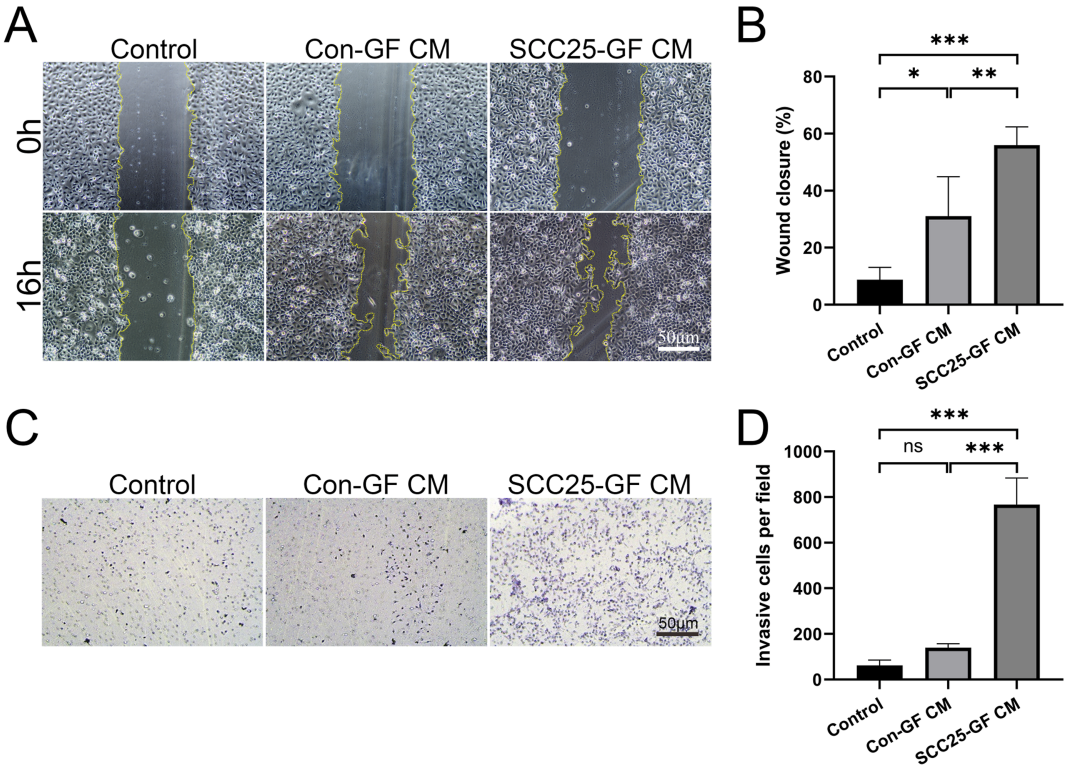

Figure 2 Analysis of migration and invasion in SCC25 cells treated with conditioned media from gingival fibroblasts. (A) Representative images from a scratch wound migration assay of SCC25 cells treated with control gingival fibroblast-conditioned medium (Con-GF CM) or SCC25-activated gingival fibroblast-conditioned medium (SCC25-GF CM) for 16 h. (B) Quantitative analysis of wound closure percentage under each treatment group. (C) Representative images of transwell invasion assay showing invasive SCC25 cells treated with either Con-GF CM or SCC25-GF CM. (D) Quantification of invaded cells per field under each treatment group. Scale bars = 50 μm. Data are presented as mean ± SD. *$P < 0.05$, **$P < 0.01$, and ***$P < 0.001$ by one-way ANOVA. Con-GF CM, conditioned medium from non-activated gingival fibroblasts; SCC25-GF CM, conditioned medium from SCC25-activated gingival fibroblasts; ns, not significant.

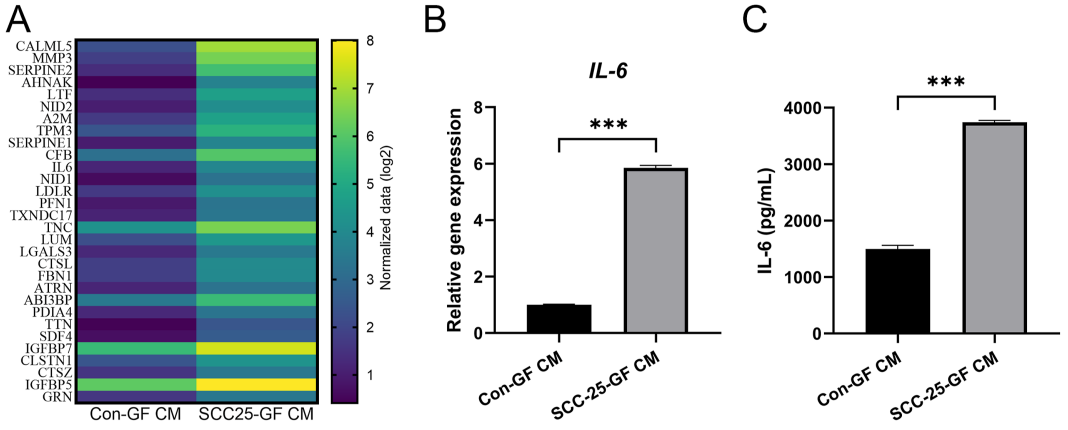

Figure 3 Secretome profiling and IL-6 expression analysis in conditioned media from gingival fibroblasts. (A) Top 30 upregulated proteins in SCC25-activated gingival fibroblast-conditioned medium (SCC25-GF CM) compared to control gingival fibroblast-conditioned medium (Con-GF CM), ranked by fold increase based on LC-MS/MS analysis. (B) Quantitative RT-qPCR analysis of *IL-6* mRNA expression in gingival fibroblasts treated with either Con-GF CM or SCC25-GF CM. (C) ELISA quantification of IL-6 protein levels in Con-GF CM and SCC25-GF CM. Data are presented as mean ± SD. ***$P < 0.001$ by Student's *t*-tests.

resulting in marker expression patterns similar to those of the control group (Fig. 4B). Immunofluorescence imaging was performed to assess the localization and expression patterns of EMT markers. In cells treated with SCC25-GF CM and control IgG, E-cadherin staining at cell–cell junctions was reduced, while N-cadherin and vimentin showed increased cytoplasmic localization. In contrast, treatment with SCC25-GF CM containing nIL-6 Ab partially restored E-

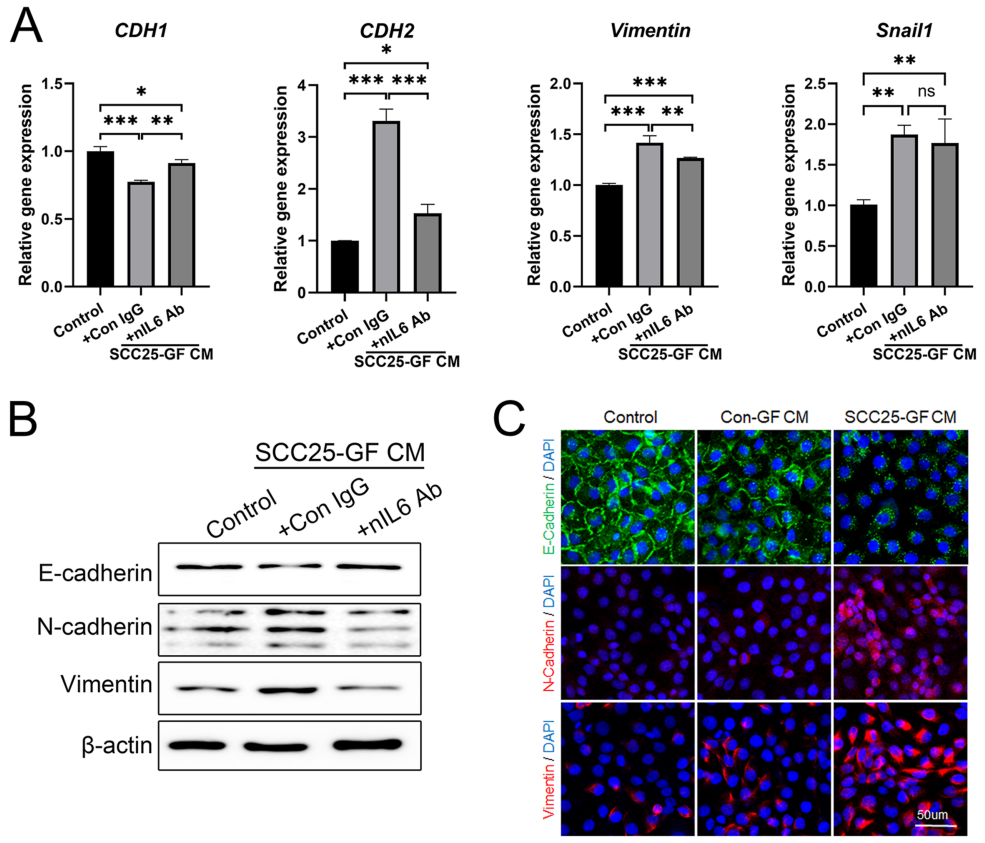

Figure 4 Effect of IL-6 depletion from SCC25-GF conditioned medium on EMT marker expression in SCC25 cells. (A) Quantitative RT-qPCR analysis of *CDH1*, *CDH2*, *Vimentin*, and *Snai1* mRNA levels in SCC25 cells treated with SCC25-GF CM supplemented with either control IgG (Con IgG) or IL-6 neutralizing antibody (nIL-6 Ab). (B) Western blot analysis of E-cadherin, N-cadherin, and vimentin protein levels under the same treatment conditions. *ACTB* was used as a loading control. (C) Immunofluorescence staining of E-cadherin, N-cadherin, and vimentin in SCC25 cells treated as indicated. Nuclei were counterstained with DAPI. Scale bars = 50 μm. Data are presented as mean ± SD. *$P < 0.05$, **$P < 0.01$, ***$P < 0.001$ by one-way ANOVA. SCC25-GF CM, conditioned medium from SCC25-activated gingival fibroblasts; nIL-6 Ab, neutralizing IL-6 antibody; ns, not significant.

cadherin localization and decreased the expression of N-cadherin and vimentin (Fig. 4C). These results confirm that IL-6 plays a pivotal role in regulating EMT marker expression in the context of SCC25-GF CM and that its inhibition effectively reverses these EMT-associated changes.

Impact of interleukin-6 blockade on migration and invasion in SCC25 cells

To examine the functional consequences of IL-6 inhibition, SCC25-GF CM-treated SCC25 cells were subjected to scratch-wound migration and invasion assays. In the scratch wound assay, SCC25-GF CM with control IgG significantly enhanced wound closure compared to the control group. However, the addition of nIL-6 Ab significantly reduced the extent of wound closure induced by SCC25-GF CM (Fig. 5A). To determine whether similar effects occur in other OSCC cell lines, we repeated the experiments using CA9-22 and HSC-3 cells. Consistent with the findings in SCC25 cells, IL-6 neutralization in these additional cell lines attenuated the upregulation of mesenchymal markers and partially restored epithelial marker expression (Fig. S1). Quantitative analysis confirmed that wound closure was markedly diminished in the nIL-6 Ab-treated group compared to the control IgG group (Fig. 5B). Similarly, in the Transwell invasion assay, SCC25-GF CM with control IgG significantly increased the number of invasive cells compared to the control group. In contrast, treatment with nIL-6 significantly reduced the invasive capacity of SCC25 cells exposed to SCC25-GF CM (Fig. 5C). Quantification of invasive cells per field revealed a marked decrease in invasiveness in the nIL-6 Ab-treated group compared to the control IgG group (Fig. 5D). These findings demonstrate that IL-6 inhibition effectively suppresses the migratory and invasive behaviors induced by SCC25-GF CM, underscoring the critical role of IL-6 in driving EMT and associated functional changes in SCC25 cells.

Discussion

The transformation of GFs into CAFs under the influence of OSCC CM highlights the dynamic interaction between cancer cells and TME. Consistent with previous studies, our findings demonstrate that CAFs derived from GF, when treated with SCC25 CM, acquire mesenchymal characteristics, as indicated by increased α-SMA and vimentin

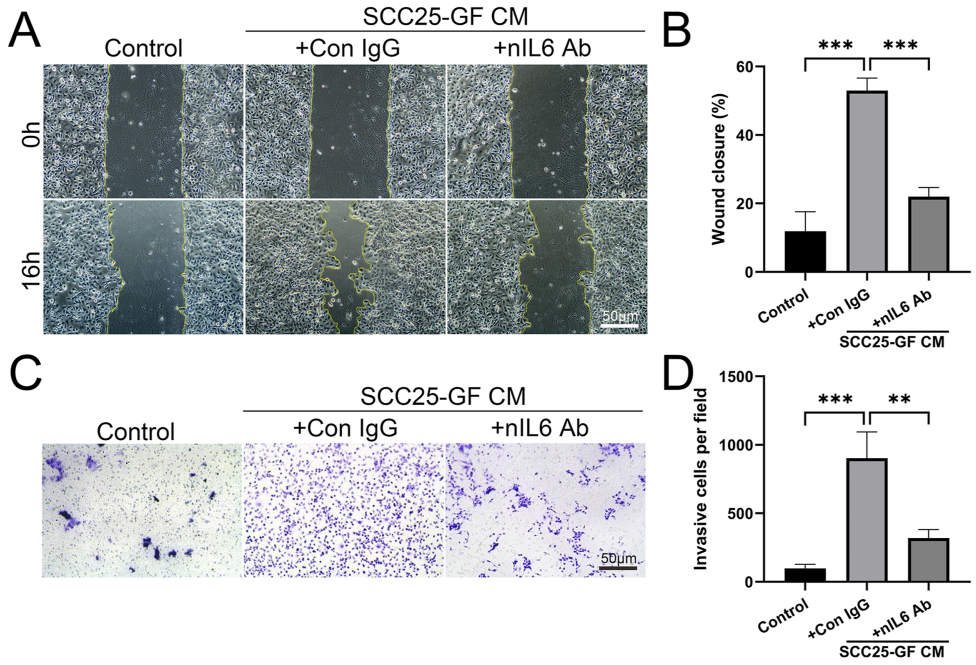

Figure 5 Effect of IL-6 depletion from SCC25-GF conditioned medium on migration and invasion of SCC25 cells. (A) Representative images of scratch wound migration assay of SCC25 cells treated with SCC25-GF CM supplemented with either control IgG (Con IgG) or neutralizing IL-6 antibody (nIL-6 Ab). (B) Quantitative analysis of wound closure percentage for each treatment group. (C) Representative images from a transwell invasion assay showing invasive SCC25 cells under the same treatment conditions. (D) Quantification of invaded cells per field in each group. Scale bars = 50 μm. Data are presented as mean ± SD. *$P < 0.01$ and **$P < 0.001$ by one-way ANOVA. SCC25-GF CM, conditioned medium from SCC25-activated gingival fibroblasts; nIL-6 Ab, neutralizing IL-6 antibody.

expression.[27,28] These CAFs secrete SCC25-GF CM, which significantly downregulates epithelial markers like E-cadherin and upregulates mesenchymal markers, including N-cadherin and Snail, in OSCC cells, thereby inducing EMT. Using secretome analysis, we expanded earlier research by identifying key CAF-derived factors that actively mediate EMT and migration. Unlike previous studies that primarily implicated ECM remodeling in CAF-mediated EMT,[29] our data emphasize the critical role of cytokines, particularly IL-6, in this process. While other CAF-derived components, such as exosomes,[30] may also contribute, our focus on IL-6 underscores its potential as a primary mediator, enhancing our understanding of stromal–tumor interaction in OSCC progression.

The identification of IL-6 as a critical cytokine driving EMT represents a significant advancement in understanding OSCC progression. Secretome analysis revealed elevated IL-6 levels in SCC25-GF CM, and functional assays confirmed that IL-6 neutralization mitigated the EMT-promoting effects of this medium. These findings are consistent with previous reports identifying IL-6 as a potent EMT inducer in various cancers, including esophageal and breast cancers.[31,32] However, our study specifically focuses on IL-6's role within the OSCC-specific TME, providing deeper insight into its mechanisms of action. Our work bridges existing gaps by demonstrating that IL-6 neutralization directly impacts EMT marker expression and functional traits such as migration and invasion. Nonetheless, further investigation is required to elucidate the downstream signaling pathways, such as STAT3, PI3K/Akt/mTOR, and MAPK/ERK,[33–35] that mediate IL-6-driven EMT in OSCC. Such mechanistic insights may pave the way for combination therapies that target both IL-6 and its downstream effectors.

EMT directly contributes to OSCC metastasis by enhancing the migratory and invasive properties of tumor cells. Our results showed that SCC25-GF CM-treated cells exhibited significantly greater migration and invasion than controls, underscoring the functional consequences of EMT induction. These findings align with clinical observations linking EMT marker expression, such as increased vimentin and N-cadherin, to advanced TNM staging and poor prognosis in OSCC patients.[36,37] By neutralizing IL-6, we demonstrated that cytokine-mediated EMT can be effectively reversed, highlighting the therapeutic potential of targeting IL-6 in OSCC. Compared to previous studies, our emphasis on the CAF-derived secretome provides a more comprehensive understanding of the interaction between stromal components and tumor cells. Although our in vitro assays robustly demonstrate the functional implications of EMT, further validation using in vivo models is necessary to assess these findings within a more complex physiological context. Nevertheless, the data presented here underscore the therapeutic potential of targeting EMT-related mechanisms in OSCC to impede disease progression.

The application of secretomics in this study offered valuable insights into the proteomic landscape of SCC25-GF CM, revealing IL-6 along with several other highly upregulated proteins. In addition to IL-6, factors such as MMP3, SERPINE2, TNC, and CTSL were markedly enriched, all of which are implicated in extracellular matrix remodeling,

cell adhesion, and invasive behavior. These findings underscore that CAF-mediated regulation of OSCC is likely driven by a network of secreted factors rather than a single cytokine. For example, MMP3 facilitates matrix degradation, SERPINE2 supports tumor cell survival, and TNC promotes structural plasticity within the tumor microenvironment, collectively suggesting synergistic interactions with IL-6 in promoting EMT and metastasis.[38,39] Future studies should aim to delineate the combined functional roles of these molecules and clarify how they interact within the CAF secretome, potentially guiding combination therapeutic strategies. Unlike previous studies that broadly examined cytokine effects,[22,40] our approach emphasizes the collective contribution of multiple secreted factors to EMT, providing a refined perspective for translational applications. Although variability in secretome composition among CAF populations remains a challenge, our results provide a strong foundation for future research into combinatorial therapies targeting multiple cytokines. Moreover, this study underscores the utility of integrating secretomics with functional assays, offering a valuable framework for identifying therapeutic targets in OSCC and other cancer types.

While the CM-based approach provided a simplified and controlled system to investigate CAF-derived factors influencing OSCC cells, it is important to acknowledge its limitations. Unlike co-culture or organoid systems, which allow dynamic and reciprocal interactions between cancer cells and stromal components, the CM model represents a unidirectional regulation. Therefore, it cannot fully replicate the bidirectional signaling and complex architecture present in the tumor microenvironment. These reciprocal interactions may involve feedback loops that influence cytokine secretion, ECM remodeling, and resistance mechanisms, which were not captured in our current model. Future studies incorporating co-culture or organoid models will be essential to validate and expand upon the findings reported here.

Declaration of competing interest

The authors declare no conflicts of interest regarding the publication of this article.

Acknowledgments

This research was supported by the National Research Foundation of Korea (NRF; Daejeon, Republic of Korea) and funded by the Korean government (Ministry of Science and ICT; Grant No. RS-2022-NR069942).

Appendix A. Supplementary data

Supplementary data to this article can be found online at https://doi.org/10.1016/j.jds.2025.08.019.

References

1. Tan Y, Wang Z, Xu M, et al. Oral squamous cell carcinomas: state of the field and emerging directions. *Int J Oral Sci* 2023;15:44.
2. Ali J, Sabiha B, Jan HU, Haider SA, Khan AA, Ali SS. Genetic etiology of oral cancer. *Oral Oncol* 2017;70:23—8.
3. Bagan J, Sarrion G, Jimenez Y. Oral cancer: clinical features. *Oral Oncol* 2010;46:414—7.
4. Sung H, Ferlay J, Siegel RL, et al. Global cancer statistics 2020: GLOBOCAN estimates of incidence and mortality worldwide for 36 cancers in 185 countries. *CA Cancer J Clin* 2021;71:209—49.
5. Zanoni DK, Montero PH, Migliacci JC, et al. Survival outcomes after treatment of cancer of the oral cavity (1985-2015). *Oral Oncol* 2019;90:115—21.
6. Ling Z, Cheng B. Tao X epithelial-to-mesenchymal transition in oral squamous cell carcinoma: challenges and opportunities. *Int J Cancer* 2021;148:1548—61.
7. Yao X, Sun S, Zhou X, Zhang Q, Guo W, Zhang L. Clinicopathological significance of ZEB-1 and E-cadherin proteins in patients with oral cavity squamous cell carcinoma. *OncoTargets Ther* 2017;10:781—90.
8. Lopez-Verdin S, Martinez-Fierro ML, Garza-Veloz I, et al. E-Cadherin gene expression in oral cancer: clinical and prospective data. *Med Oral Patol Oral Cir Bucal* 2019;24:e444—51.
9. Afrem MC, Margaritescu C, Craitoiu MM, Ciuca M, Sarla CG. Cotoi OS the immunohistochemical investigations of cadherin "switch" during epithelial-mesenchymal transition of tongue squamous cell carcinoma. *Rom J Morphol Embryol* 2014;55:1049—56.
10. Sawant SS, Vaidya M, Chaukar DA, et al. Clinical significance of aberrant vimentin expression in oral premalignant lesions and carcinomas. *Oral Dis* 2014;20:453—65.
11. de Freitas Silva BS, Yamamoto-Silva FP, Pontes HA. Pinto junior Ddos S E-cadherin downregulation and Twist overexpression since early stages of oral carcinogenesis. *J Oral Pathol Med* 2014;43:125—31.
12. Bienkowska KJ, Hanley CJ, Thomas GJ. Cancer-associated fibroblasts in oral cancer: a current perspective on function and potential for therapeutic targeting. *Front Oral Health* 2021;2:686337.
13. Wu MH, Hong HC, Hong TM, Chiang WF, Jin YT, Chen YL. Targeting galectin-1 in carcinoma-associated fibroblasts inhibits oral squamous cell carcinoma metastasis by downregulating MCP-1/CCL2 expression. *Clin Cancer Res* 2011;17:1306—16.
14. Datar UV, Kale AD, Angadi PV, Hallikerimath S, Deepa M, Desai KM. Role of cancer-associated fibroblasts in oral squamous cell carcinomas, surgical margins, and verrucous carcinomas: an immunohistochemical study. *J Clin Transl Res* 2022;8:80—5.
15. Arebro J, Lee CM, Bennewith KL. Garnis C cancer-associated fibroblast heterogeneity in malignancy with focus on oral squamous cell carcinoma. *Int J Mol Sci* 2024;25:1300.
16. Zhang JY, Zhu WW, Wang MY, et al. Cancer-associated fibroblasts promote oral squamous cell carcinoma progression through LOX-Mediated matrix stiffness. *J Transl Med* 2021;19:513.
17. Heo SC, Nam IH, Keum BR, Yun YG, Lee JY, Kim HJ. C-X-C motif chemokine ligand 1 derived from oral squamous cell carcinoma promotes cancer-associated fibroblast differentiation and tumor growth. *Mol Biomed* 2025;6:40.
18. Xu J, Lamouille S, Derynck R. TGF-beta-induced epithelial to mesenchymal transition. *Cell Res* 2009;19:156—72.
19. Li CW, Xia W, Huo L, et al. Epithelial-mesenchymal transition induced by TNF-alpha requires NF-kappaB-mediated transcriptional upregulation of Twist1. *Cancer Res* 2012;72:1290—300.
20. Li S, Lu J, Chen Y, et al. MCP-1-induced ERK/GSK-3beta/Snail signaling facilitates the epithelial-mesenchymal transition and promotes the migration of MCF-7 human breast carcinoma cells. *Cell Mol Immunol* 2017;14:621—30.
21. Chen CJ, Sung WW, Lin YM, et al. Gender difference in the prognostic role of interleukin 6 in oral squamous cell carcinoma. *PLoS One* 2012;7:e50104.

22. Yadav A, Kumar B, Datta J, Teknos TN. Kumar P IL-6 promotes head and neck tumor metastasis by inducing epithelial-mesenchymal transition via the JAK-STAT3-SNAIL signaling pathway. *Mol Cancer Res* 2011;9:1658—67.
23. Gyamfi J, Lee YH, Eom M, Choi J. Interleukin-6/STAT3 signalling regulates adipocyte induced epithelial-mesenchymal transition in breast cancer cells. *Sci Rep* 2018;8:8859.
24. Ara T, Declerck YA. Interleukin-6 in bone metastasis and cancer progression. *Eur J Cancer* 2010;46:1223—31.
25. Zhao Y, Shen M, Wu L, et al. Stromal cells in the tumor microenvironment: accomplices of tumor progression? *Cell Death Dis* 2023;14:587.
26. Gopinathan G, Milagre C, Pearce OM, et al. Interleukin-6 stimulates defective angiogenesis. *Cancer Res* 2015;75:3098—107.
27. Kalluri R. The biology and function of fibroblasts in cancer. *Nat Rev Cancer* 2016;16:582—98.
28. Attieh Y, Vignjevic DM. The hallmarks of CAFs in cancer invasion. *Eur J Cell Biol* 2016;95:493—502.
29. Hanahan D, Coussens LM. Accessories to the crime: functions of cells recruited to the tumor microenvironment. *Cancer Cell* 2012;21:309—22.
30. Kalluri R. The biology and function of exosomes in cancer. *J Clin Investig* 2016;126:1208—15.
31. Ebbing EA, van der Zalm AP, Steins A, et al. Stromal-derived interleukin 6 drives epithelial-to-mesenchymal transition and therapy resistance in esophageal adenocarcinoma. *Proc Natl Acad Sci U S A* 2019;116:2237—42.
32. Sullivan NJ, Sasser AK, Axel AE, et al. Interleukin-6 induces an epithelial-mesenchymal transition phenotype in human breast cancer cells. *Oncogene* 2009;28:2940—7.
33. Johnson DE, O'Keefe RA, Grandis JR. Targeting the IL-6/JAK/STAT3 signalling axis in cancer. *Nat Rev Clin Oncol* 2018;15:234—48.
34. Wegiel B, Bjartell A, Culig Z, Persson JL. Interleukin-6 activates PI3K/Akt pathway and regulates cyclin A1 to promote prostate cancer cell survival. *Int J Cancer* 2008;122:1521—9.
35. Okitsu K, Kanda T, Imazeki F, et al. Involvement of interleukin-6 and androgen receptor signaling in pancreatic cancer. *Genes Cancer* 2010;1:859—67.
36. Thiery JP, Acloque H, Huang RY, Nieto MA. Epithelial-mesenchymal transitions in development and disease. *Cell* 2009;139:871—90.
37. Costa LC, Leite CF, Cardoso SV, et al. Expression of epithelial-mesenchymal transition markers at the invasive front of oral squamous cell carcinoma. *J Appl Oral Sci* 2015;23:169—78.
38. Valiente M, Obenauf AC, Jin X, et al. Serpins promote cancer cell survival and vascular co-option in brain metastasis. *Cell* 2014;156:1002—16.
39. Kessenbrock K, Plaks V, Werb Z. Matrix metalloproteinases: regulators of the tumor microenvironment. *Cell* 2010;141:52—67.
40. Bhat AA, Nisar S, Maacha S, et al. Cytokine-chemokine network driven metastasis in esophageal cancer; promising avenue for targeted therapy. *Mol Cancer* 2021;20:2.